

The Effect of Multiple Cation (Al, Si, Ti, Co) Doping on Electrochemical Performance of LiMn_2O_4 Cathode Active Material

F. KILIÇ DOKAN*, H. ŞAHAN, S. VEZİROĞLU, N. AKKUŞ TAŞ, A. AYDIN AND Ş. PATAT

Department of Chemistry, Faculty of Science, Erciyes University, Kayseri, 38039, Turkey

In order to improve the cycling performance of LiMn_2O_4 , the spinel phases base and multiple cation doped $\text{LiMn}_{1.95}\text{Al}_{0.0125}\text{Si}_{0.0125}\text{Ti}_{0.0125}\text{Co}_{0.0125}\text{O}_4$, $\text{LiMn}_{1.9}\text{Al}_{0.025}\text{Si}_{0.025}\text{Ti}_{0.025}\text{Co}_{0.025}\text{O}_4$ spinels were synthesized by the glycine–nitrate combustion process. The structures of the products were investigated by X-ray diffraction, scanning electron microscopy and electrochemical tests.

DOI: 10.12693/APhysPolA.123.365

PACS: 88.80.ff

1. Introduction

Spinel LiMn_2O_4 has been extensively studied as the most promising cathode material for lithium-ion batteries because of its low cost, acceptable environmental characteristics, and good safety as compared to layered oxides such as LiCoO_2 and LiNiO_2 [1–3]. However, the capacity of LiMn_2O_4 fades during cycling for several reasons, such as an instability of an organic-base electrolyte in a high potential region [4], the dissolution of manganese into electrolyte [5, 6], change in crystal lattice arrangement with cycling [7], and others.

Much effort has been made by the international lithium battery community to minimize the capacity fading of spinel electrode. Two main approaches have been used to address this problem; partial substitution of manganese ions by tri, di or mono valent cations like [8] Al, Mg, Cr, Co and Li or coating the spinel particles with a protective layer such as LBO [8], CaCO_3 [9]. Herein, we report the synthesis and characterization of multiple cation doping on electrochemical performance of LiMn_2O_4 cathode active material.

Up to now, the most important factor seems to be the onset of the tetragonal distortion associated with the Jahn–Teller effect in deeply discharged LiMn_2O_4 electrodes. To improve the stability, doping of the cubic LiMn_2O_4 with iso-or aliovalent cations has been done [10–13]. These dopants substitute manganese placed at the 16(d) octahedral position of the $Fd3m$ space group and prevents the Jahn–Teller distortion in the 4 V plateau by increasing the average oxidation state of the manganese above +3.5. The effect of dopants (Me) on the electrochemical characteristics of the $\text{LiMe}_y\text{Mn}_{2-y}\text{O}_4$ spinels has been very much studied.

Recent work has shown that, when the Mn concentration in the spinel material is reduced by the addition of appropriate dopants, improved cycling stability in the

4 V range could be achieved [8] have shown that the substitution of M ions at the Mn site increases the average valence of Mn, and thus decreases the number of the Jahn–Teller Mn^{3+} ions.

2. Experimental

Untreated LiMn_2O_4 and multiple cation doped $\text{LiMn}_{1.95}\text{Al}_{0.0125}\text{Si}_{0.0125}\text{Ti}_{0.0125}\text{Co}_{0.0125}\text{O}_4$, $\text{LiMn}_{1.9}\text{Al}_{0.025}\text{Si}_{0.025}\text{Ti}_{0.025}\text{Co}_{0.025}\text{O}_4$ spinels were prepared by a glycine–nitrate combustion process [14]. Firstly, stoichiometric amounts of the raw materials were dissolved in distilled water, Li_2CO_3 (Merck), $\text{Mn}(\text{CH}_3\text{COO})_2 \cdot 4\text{H}_2\text{O}$ (Sigma), $\text{Co}(\text{NO}_3)_2 \cdot 6\text{H}_2\text{O}$ (Surechem Products), and then TEOS (Merck), $\text{Ti}[\text{O}(\text{CH}_2)_3\text{CH}_3]_4$ (Aldrich), glycine (Merck) was added to the solution either as a solid or as a water solution. Its role was to serve both as a fuel for combustion and as a complexant to prevent inhomogeneous precipitation of individual components prior to combustion. Finally, nitric acid with the same mole of acetate anions was added to the solution. The molar ratio of glycine to nitrate was 1:4. The solution was heated continuously without any previous thermal dehydration. Afterwards the solution became transparent viscous gel which auto-ignited automatically, giving a voluminous, black, sponge-like ash product of combustion. The resulting ash was heated at 800 °C for 12 h.

The phase identification and the evaluation of lattice parameters of the LiMn_2O_4 and multiple cation doped samples powders were carried out by powder X-ray diffraction (XRD) using copper $\text{Cu } K_\alpha$ radiation (Bruker AXS D8). The particle morphology of the powders was examined by means of scanning electron microscopy (SEM) (LEO 440), operated at 20 kV.

The electrochemical studies were carried out in two-electrode teflon cells. The cells were fabricated by using the synthesis samples as a cathode and lithium foil as anode. A glass fiber separator soaked in electrolyte separated the two electrodes. The electrolyte consisted of 1 M solution of LiPF_6 dissolved in an ethylene carbon-

*corresponding author; e-mail: fatmainorg@hotmail.com

ate (Aldrich)/diethyl carbonate (Merck) (EC/DEC, 1:1 ratio by volume). For the preparation of the cathode composite, a slurry mixed with 85 wt% of cathode active material, 10 wt% of acetylene black conductor (Alfa Aesar) and 5 wt% of polyvinylidene fluoride (PVDF, Fluka) binder in 1-methyl-2-pyrrolidinone (NMP, Merck) was pasted on aluminum foil current collector with a diameter of 13 mm, followed by vacuum drying at 120 °C for overnight in a vacuum oven and uniaxial pressing between two flat plates at 2 ton for 5 min. The electrode loading was about 4 mg of cathode active material. Charge–discharge tests were performed galvanostatically at a current rate of 1 C with cut-off voltages of 3.5–4.45 V (versus Li/Li⁺) at room temperature in a multi-channel battery tester (VersaSTAT MC).

3. Result and discussion

The XRD patterns of all powders are presented in Fig. 1. The XRD pattern of the base LiMn₂O₄ powders shows that the material is pure spinel phase with the crystal lattice parameter of 8.235 Å, 8.227 Å, 8.222 Å. The spectrum of LiMn_{1.9}Al_{0.0125}Si_{0.0125}Ti_{0.0125}Co_{0.0125}O₄ and LiMn_{1.9}Al_{0.025}Si_{0.025}Ti_{0.025}Co_{0.025}O₄ is almost the same as that of the base one. The absence of any other peaks in the XRD patterns of doped LiMn₂O₄ samples indicates that there are no else phases in the obtained doped samples as compared with pure spinel LiMn₂O₄.

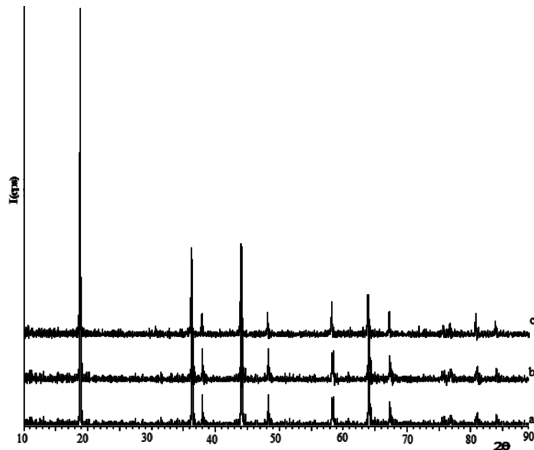


Fig. 1. XRD patterns of the (a) LiMn₂O₄, (b) LiMn_{1.9}Al_{0.0125}Si_{0.0125}Ti_{0.0125}Co_{0.0125}O₄, (c) LiMn_{1.9}Al_{0.025}Si_{0.025}Ti_{0.025}Co_{0.025}O₄.

SEM photographs of all powders are presented in Fig. 2. The photographs show that the particle size becomes smaller and the size distribution becomes much narrower with substituting of metal ions for the Mn³⁺.

Since electrochemical lithium intercalation and deintercalation are limited by the rate of diffusion, the surface morphology and particle size distribution are the important factors for cycling performance of the Li ion batteries. Smaller grain size and narrower particle size distribution can favor the lithium ion mobility in the particles

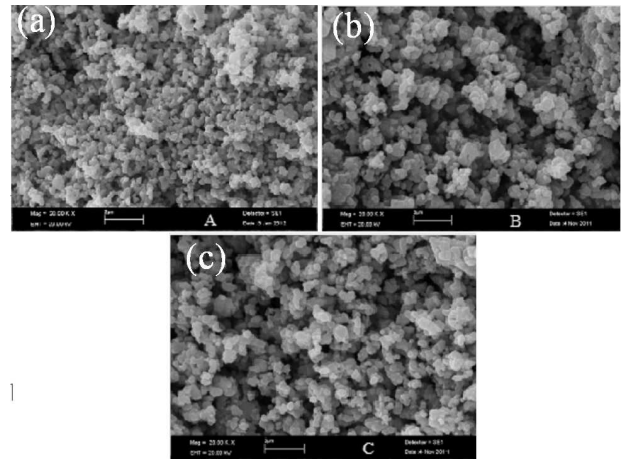


Fig. 2. SEM photographs of (A) bare LiMn₂O₄, (B) LiMn_{1.9}Al_{0.0125}Si_{0.0125}Ti_{0.0125}Co_{0.0125}O₄, (C) LiMn_{1.9}Al_{0.025}Si_{0.025}Ti_{0.025}Co_{0.025}O₄.

by reducing the ion diffusion pathway [15]. According to the scanning electron microscopy results it is apparent that samples have fine particles and homogeneous particle distribution (Fig. 2). It is commonly accepted that good morphology and uniform particle size distribution are very important for both high specific capacity and good cycleability of the cathode material for lithium ion battery [16].

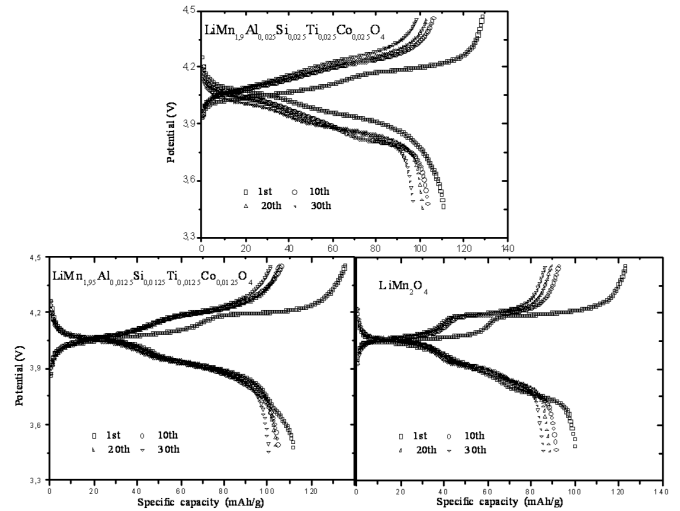


Fig. 3. Continuous charge-discharge curves during 30 cycles.

Figure 3 shows voltage and discharge capacity curves for various charge–discharge cycles in the voltage range 3.5–4.45 V at room temperature. The cells were first activated by charging up to 4.45 V and then discharging to 3.5 at room temperature.

After 30 cycles, the discharge capacity of the LiMn₂O₄ decayed to 99.9 and the loss of capacity was about 14.40%. The discharge capac-

ity of $\text{LiMn}_{1.95}\text{Al}_{0.0125}\text{Si}_{0.0125}\text{Ti}_{0.0125}\text{Co}_{0.0125}\text{O}_4$ and $\text{LiMn}_{1.9}\text{Al}_{0.025}\text{Si}_{0.025}\text{Ti}_{0.025}\text{Co}_{0.025}\text{O}_4$ reached 111.8 and 110.59 mAh/g, and the discharge capacity fade was 9.93 and 12.57%, respectively (Fig. 3). It is apparent that the discharge capacity of the $\text{LiMn}_{1.95}\text{Al}_{0.0125}\text{Si}_{0.0125}\text{Ti}_{0.0125}\text{Co}_{0.0125}\text{O}_4$, $\text{LiMn}_{1.9}\text{Al}_{0.025}\text{Si}_{0.025}\text{Ti}_{0.025}\text{Co}_{0.025}\text{O}_4$ composition is more stable than that of the LiMn_2O_4 .

4. Conclusions

In this study we reported that the effect of the multiple cation doped on electrochemical properties of LiMn_2O_4 has been studied by using electrochemical tests and XRD, SEM, We observed that multiple cation substitution for Mn has a significant effect on the electrochemical cycling performance. The Mn^{3+} content decrease due to substitution of multiple metal ions on the LiMn_2O_4 framework causes changes in the local ordering. It is clear from these results that the Jahn–Teller distortion in samples is suppressed by multiple metal ions. In addition, multiple metal ions enhance the stability of the octahedral sites in spinel skeleton structure because the bonding energy of the doped metal oxygen is stronger than that of Mn–O (402 kJ/mol) [17].

Acknowledgments

This research has been supported by the Scientific and Technological Research Council of Turkey (Project No. 109T811).

References

- [1] J.M. Tarascon, E. Wang, F.K. Shokoohi, W.R. McKinnon, S. Colson, *J. Electrochem. Soc.* **138**, 2859 (1991).
- [2] J.M. Tarascon, D. Guyomard, *Electrochim. Acta* **38**, 1221 (1993).

- [3] R.J. Gummow, A. de Kock, M. Thackeray, *Solid State Ionics* **69**, 59 (1994).
- [4] Y. Xia, Y. Zhou, M. Yoshio, *J. Electrochem. Soc.* **144**, 2593 (1997).
- [5] S.T. Myung, S. Komaba, N. Kumagai, *J. Electrochem. Soc.* **148**, A482 (2001).
- [6] P. Arora, B.N. Popov, R.E. White, *J. Electrochem. Soc.* **145**, 807 (1998).
- [7] L. Guohua, H. Ikuta, T. Uchida, M. Wakihara, 10.1149/1.1836405 *J. Electrochem. Soc.* **143**, 178 (1996).
- [8] H. Şahan, H. Göktepe, Ş. Patat, A. Ülgen, *Solid State Ionics* **178**, 1837 (2008).
- [9] H. Şahan, H. Göktepe, Ş. Patat, *J. Mater. Sci. Technol.* **27**, 415 (2011).
- [10] G. Pistoia, A. Antonini, R. Rosati, C. Bellitto, G.M. Ingo, *Chem. Mater.* **9**, 1443 (1997).
- [11] J.M. Tarascon, E. Wang, F.K. Sho koochi, W.R. McKinnon, S. Colson, *J. Electrochem. Soc.* **138**, 2859 (1991).
- [12] D. Song, H. Ikuta, T. Uchida, M. Wakihara, *Solid State Ionics* **117**, 151 (1999).
- [13] M.Y. Song, D.S. Ahn, S.G. Kang, S.H. Chang, *Solid State Ionics* **111**, 237 (1998).
- [14] Y. Zhang, H.C. Shin, J. Dong, M. Liu, *Solid State Ionics* **171**, 25 (2004).
- [15] C.M. Julien, K. Zaghib, *Electrochim. Acta* **50**, 411 (2004).
- [16] Y.P. Fu, Y.H. Su, C.H. Lin, *Solid State Ionics* **166**, 137 (2004).
- [17] L. Guohua, H. Ikuta, T. Uchida, M. Wakihara, *J. Electrochem. Soc.* **143**, 178 (1995).